Determination of ion and neutral deposition rates using a quartz crystal microbalance and a gridded energy analyzer

K. Zaidi and D. Gahan

INTRODUCTION

This application note describes the design and calibration of a quartz crystal microbalance with added gridded energy analyzer for measurement of ion and neutral deposition rates in plasma processes. The purpose of this note is to give a background overview of this technology before introducing the theory of operation of the Quantum system, a commercially available product based on this concept.

Common processes for the metallisation of semiconductor wafers are Chemical Vapour Deposition (CVD) and Physical Vapour Deposition (PVD). Both techniques have their limitations and struggle to maintain the demands of the industry. CVD is effective for producing high purity thin films with excellent crystalline structures for many materials. When depositing aluminium, however, CVD struggles to fill entire trench volumes or vias. The standard PVD techniques for metal deposition (sputtering and evaporation) can fill these features but does not provide good step coverage for high aspect-ratio (AR) trenches and vias when depositing aluminium for example.

To make sputtering a feasible mechanism for filling high AR trenches, several techniques have been investigated; including collimated sputtering and ionized sputtering.
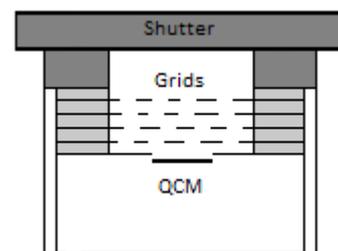

Figure 1. Simplified schematic of the QCM with added GEA developed by Green et al[2].

Rossnagel et al[1] have filled trenches with AR = 3 using these techniques, however, there are still some drawbacks. Only atoms travelling with ± 5° of normal incidence to the substrate can pass through the collimator. The collimators tend to clog, thus decreasing the flux on the substrate. Furthermore, the deposition that builds up on the sides of the collimator tends to flake off[1].

Ionized sputtering achieves a directional flux by ionizing the metal atoms sputtered from the target. A bias applied to the substrate is then used to accelerate the metal ions straight down into the trenches and vias. The particles that reach the substrate include directed ions and isotropic neutrals, and can fill high AR trenches.

In the work by Green et al[2] an in-situ method for determining the flux ionization fraction using a quartz crystal microbalance (QCM) and a gridded energy analyser (GEA) was developed. The GEA was located
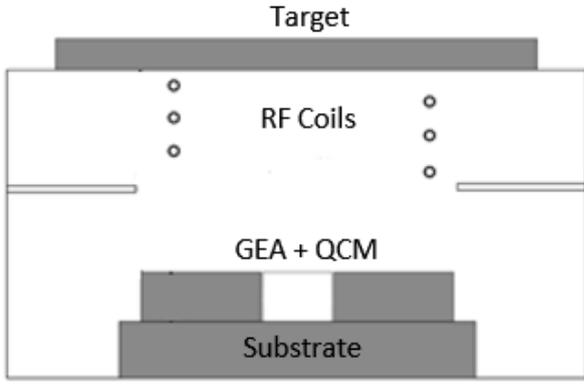
Figure 2. Schematic of the magnetron sputtering machine used by Green et al[2]

Figure 3. Graph of the geometric factor (G) versus the aspect ratio (l/w). We also show the aspect ratio (AR) and resulting G factor for the Quantum system.

above the QCM and biased at a potential either to admit or to repel the ions arriving from the plasma.

When the grids are biased negatively, both ions and neutrals produced in the system arrive at the QCM, and when the grids are biased sufficiently positively, only neutrals reach the QCM[2]. This allows the determination of the ionization fraction of the metal flux.

A three-grid GEA was positioned directly above a QCM. Each grid consists of a mesh of stainless steel wire of approximately 52% open area. Each grid was mounted on a Teflon disk. The Teflon disk provides a sturdy support for the grids whilst insulating the grids from each other. Each grid can be biased independently and their currents can be measured separately. As shown in figure 1, an aluminium casing houses the GEA and QCM. A shutter is also provided to protect the instrument from the initial sputter clean and from plasma deposition when the diagnostic is not in use.

The instrument was positioned approximately 166 mm below the target. The rf coils that ionize the aluminium ejected from the target surface, are located between the substrate and target, shown in figure 2.

CALIBRATION

Calibration of the instrument is very important. It enables a correlation to be determined between deposition rate on the substrate surface and that of the QCM beneath the grids.
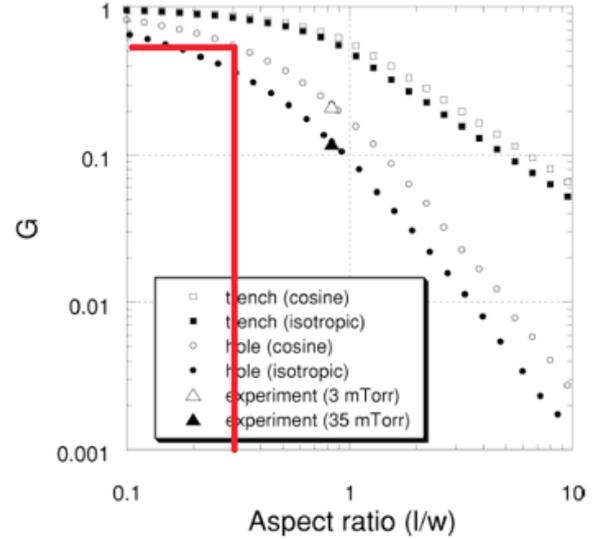
The fraction of flux that reaches the QCM though the instrument stack was determined empirically and is referred to as the geometric factor, G, which is a function of pressure. Taking the geometric factor and the grid transparency into account, the QCM deposition rate is given by:

$$R_{sensor} = R_{substrate} G \left(T_g \right)^n \qquad (1)$$

where R_{sensor} is the deposition rate at the QCM, $R_{substrate}$ is the deposition rate at the substrate, T_g is the grid transparency, and n is the number of grids used in the sensor configuration.

Comparison of the deposition on the QCM to the deposition on the substrate allowed the effect on the deposition due to geometry and scattering to be determined. A model was also developed to predict the effect of the geometry on the flux received at the QCM. Since the actual QCM lies at the bottom of a cylindrical hole in the casing, its surface is shadowed by the casing walls and is partially shielded from the plasma above.

A calculation was presented which assumes an isotropic flux of particles in the region of the crystal. This calculation corresponds to a high-pressure condition where scattering in the chamber is significant.
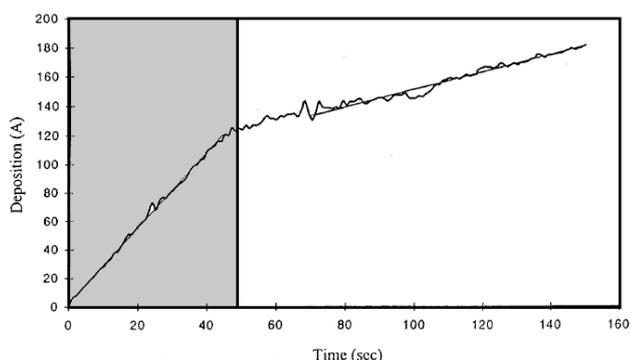
Figure 4. Total deposition versus time for neutrals plus ions and for neutrals only.

To demonstrate how this type of instrument works and the type of data produced an experiment was carried out. The magnetron power was set to 2 kW and an aluminium target was used. The rf coil power was set to 160 W to ionise the metal ions. Discharge pressure was set to 35 mTorr. A dc bias of -30 V was applied to the substrate, including the sensor. Therefore, grid 1 and grid 3 were also biased at -30 V. Grid 2 is biased to either repel all positive ions or admit all positive ions through to the crystal for detection.

The result of this experiment is shown in figure 4. The deposition rate is clearly much higher when both ions and neutrals are collected. The actual deposition rates are determined by finding the slope of a straight line fit to the deposition versus time data. In this experiment the neutral plus ion deposition rate was approximately 2.7 Å/s while the neutral only deposition rate is approximately 0.6 Å/s.

Another calculation was performed for an infinitely long trench of rectangular cross section, using both an isotropic flux distribution and a cosine flux distribution. This corresponds to the distribution of the sputter flux as it leaves the sputter target. The cosine distribution can be used at low pressure where scattering is negligible. The model is solved for both cylindrical hole and rectangular trench with AR defined as length divided by the width (*l/w*).

Figure 3 shows *G* as a function of AR for both hole and trench for cosine and isotropic distributions, along with experimentally measured data. These experimental data points perfectly match the cosine and isotropic distributions for low and high pressure operation respectively (at this point no grids were in place). As AR approaches 0, the flux factor approaches 1, indicating that the flux on the crystal is equal to that on the top surface, as expected.

For the calibration performed at 3 mTorr, grids were placed on the QCM. Using equation (1), with one, two and three grids the sensor deposition rate is expected to be 6.4%, 3.4%, and 1.8% of the substrate deposition rate, respectively. The actual deposition rates measured at the QCM are in very good agreement with the deposition rates predicted by theory. This result provides an accurate means for determining calibration coefficients for other designs with different AR and grid transparencies.

The Quantum system is calibrated directly from figure 3, where the red line indicates the AR of the design and the resulting G factor used for geometrical shadowing of the neutrals.

SUMMARY

In summary, this application note introduces the background technology in relation to the design and calibration of a QCM with added GEA. The methodology and analytical model developed provides an extremely useful tool for calibrating the deposition rates at the substrate surface from the measurements made at the crystal. The commercial Quantum system, which will be introduced in the next technical note in this series, utilises a similar calibration methodology.

REFERENCES

[1] S. M. Rossnagle, D. Mikalsen, H. Kinoshita, and J. J. Cuomo, J. Vac. Sci. Technol. A, **9**, 261 (1991).

[2] K. M. Green, D. B. Hayden, D. R. Juliano and D. N. Ruzic, Rev. Sci. Instrum. **68**, 4555 (1997).